Hugoniot data of plastic foams obtained from laser-driven shocks

R. Dezulian, F. Canova, S. Barbanotti, F. Orsenigo, R. Redaelli, T. Vinci, G. Lucchini, and D. Batani
Dipartimento di Fisica "G. Occhialini," Università degli Studi di Milano Bicocca, Piazza della Scienza 3, 20126 Milano, Italy

B. Rus, J. Polan, M. Kozlová, M. Stupka, A. R. Praeg, P. Homer, T. Havlicek, M. Soukup, E. Krousky, J. Skala, R. Dudzak, and M. Pfeifer
PALS Research Centre, Za Slovankou 3, 18221 Prague 8, Czech Republic

H. Nishimura, K. Nagai, F. Ito, and T. Norimatsu
ILE, Osaka University, 2-6 Yamadaoka, Suita City, Osaka 565-0871, Japan

A. Kilpio, E. Shashkov, I. Stuchebrukhov, V. Vovchenko, V. Chernomyrdin, and I. Krasuyk
General Physics Institute, Russian Academy of Sciences, Moscow, Russia
(Received 16 August 2005; revised manuscript received 22 November 2005; published 10 April 2006)

In this paper we present Hugoniot data for plastic foams obtained with laser-driven shocks. Relative equation-of-state data for foams were obtained using Al as a reference material. The diagnostics consisted in the detection of shock breakout from double layer Al/foam targets. The foams [poly(4-methyl-1-pentene) with density $130>\rho>60$ mg/cm^3] were produced at the Institute of Laser Engineering of Osaka University. The experiment was performed using the Prague PALS iodine laser working at 0.44 μm wavelength and irradiances up to a few 10^{14} W/cm^2. Pressures as high as 3.6 Mbar (previously unreached for such low-density materials) where generated in the foams. Samples with four different values of initial density were used, in order to explore a wider region of the phase diagram. Shock acceleration when the shock crosses the Al/foam interface was also measured.

DOI: 10.1103/PhysRevE.73.047401 PACS number(s): 52.50.Jm, 52.35.Tc

INTRODUCTION

Low-density foam layers have the potential of allowing the improvement of target design in ICF [1]. This is the main motivation explaining the recent large interest in laser-plasma experiments using foam targets. Indeed, laser imprint may be strongly reduced by thermal smoothing in a relatively thick, hot, low-density (but overcritical) outer foam layer of ICF targets [2]. Alternatively, very-low-density (undercritical, thin and transparent) foams may reduce the imprint problem by acting as dynamic phase plates [3]. Moreover, density tailoring of complex targets including a foam layer may help to suppress the growth of Rayleigh-Taylor instability [4]. Apart from direct use in ICF targets, foams have been used in EOS experiments to increase pressure due to impedance mismatch on foam-solid interface [5], and finally they are important in astrophysics-dedicated experiments [6].

Due to such large interest, there is a need for a precise characterization of foam materials under the action of intense laser light, which implies the generation of strong pressures (in the Megabar range) and, in particular, there is need for getting equation-of-state (EOS) data for foams along the Hugoniot, i.e., under the action of an intense shock. In this context, a few experiments have been performed either by using conventional shocks [7], or laser-generated shocks [8]. However there is certainly the need for more data (due to the variety of foam materials, as well as the large pressure range of interest), and for improving the experimental methods for EOS determination along the Hugoniot, which are the two goals of the present report. Apart from a few technical details, which will be discussed in the following, our method is based on the impedance mismatch technique, already discussed in details in Ref. [9] and the use of an Al target as a reference material: the determination of the shock velocity in Al allows to get the shock pressure via the EOS model (here we used the well-known Sesame tables [10]).

EXPERIMENTAL SETUP

The experiment was performed with the iodine laser of PALS [11], which delivers a single beam, 29 cm in diameter, with energies up to 250 J per pulse at 0.44 μm. The laser pulse is Gaussian in time with a full width at half-maximum (FWHM) of 350 ps. The schematic experimental setup is similar to the one used in Ref. [12] and shown in Fig. 1. The focusing lens had a focal length $f=600$ mm ($f/2$ aperture). A blue filter before the entrance window did cut ω and 2ω

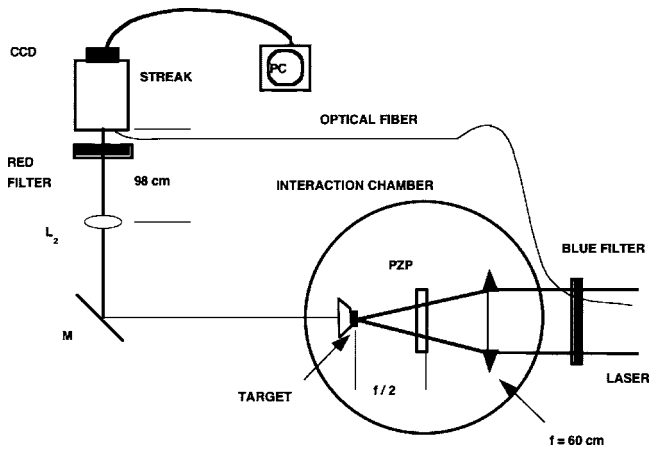

FIG. 1. Experimental setup at PALS.

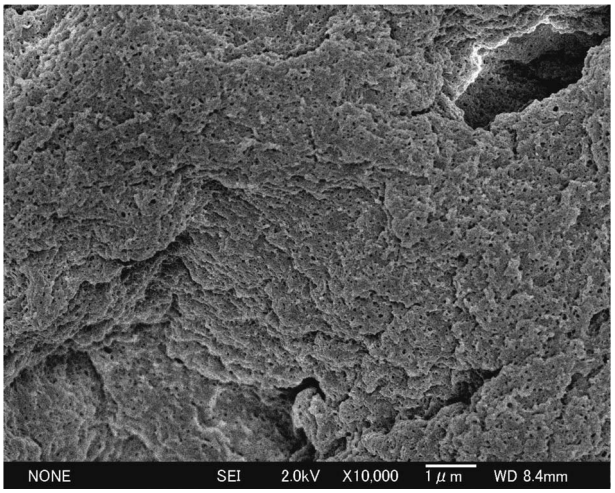

FIG. 2. Scanning electron microscope image of the foams produced at ILE and used in the experiment.

light. The diagnostics used to detect the shock breakout from the target rear face consisted in a pair of lenses imaging the rear face onto the slit of a streak camera (Hamamatsu C7700 with S-1 photocathode). The first one was a complex $f/2$ objective, with $f=100$ mm, producing a parallel beam between the two lenses. A red filter RG60 before the streak camera cut out any 3ω light. The second lens had $f=98$ cm, giving a total optical magnification $M=9.8$. The CCD had 512×512 pixel and 16 bits dynamic range. The spatial resolution was measured to be 2.6 μm/pixel, and the temporal resolution 3.12 ps/pixel (choosing a 1600 ps time window).

The primary condition of producing high quality flat shocks imposed the use of phase zone plates (PZP) [13]. The PZP, half of the laser beam size, was placed at $f/2$ from target. The characteristics of our optical system (PZP+focusing lens) implied a focal spot of 560 μm FWHM, with a 400 μm flat central region, corresponding to peak intensities up to 2.4×10^{14} W/cm^2.

TARGET PRODUCTION

Our plastic foams were produced at the Target Material Laboratory of ILE, Osaka University, by the aerogel method, which allows the production of films with area of mm^2 order and density in the range from 50 to 150 mg/cm^3 with chemical composition CH_2 (poly(4-methyl-1-pentene)). Several-ten-nanometer sized crystals are aggregated, and macroscopic-pore void size was $\leqslant2$ μm over an area <1 mm^2 and for density >50 mg/cm^3 [14] (see Fig. 2). The foam film was put in contact with the aluminum foil using the single molecule glue method [14].

In the experiment, we used three-layer targets. The first layer was a 4 μm plastic (CH) ablator, which was present to reduce preheating [15]. The second was a 10 μm Al foil followed by a foam layer of typical thickness 100–190 μm (the foam thickness was measured on each single sample). Such a foam layer was finally covered on half size by a thin (500 Å) Al deposition.

Our foams are transparent to visible light, and here we used their transparency to detect a shock breakout from the Al base through the foam (as previously done in Ref. [8]).

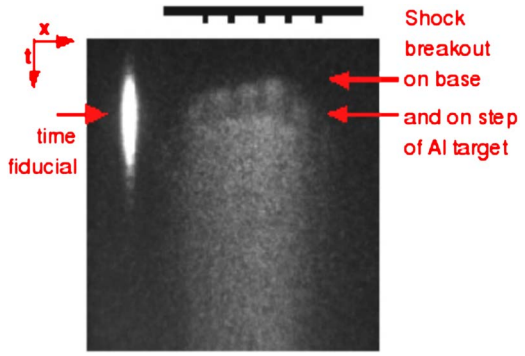

FIG. 3. (Color online) Shock breakout image from an Al stepped target for laser energy $E_L=229$ J (target scheme on the top). The dimensions of the images are 1.60 ns $\times$ 1300 μm. Times flows up to down. The time delay between base and step is $\Delta t=169$ ps giving a shock velocity $D=29.6$ μm/ns. The time fiducial on the up-left part of the image is a reference for the laser pulse arrival on target front. The early signals (the *fingers* in the image) correspond to breakout from the base of the *comb* target.

However, unlike in that experiment, we did use quite thick foam layers (typically $\approx100-190$ μm against ≈20 μm). Indeed, provided the shock velocity is constant in the foam (i.e., the shock is stationary), the uncertainty in the measurement of the shock velocity in the foam is inversely proportional to the foam thickness. However, in this case it became impossible to use an Al stepped target as reference (as done in Ref. [8]). In fact, with thin steps (5–10 μm as in Ref. [8]) the time difference between breakout at base and step is not easily detectable on the same streak image of the foam shock breakout. On the other side, using thick steps would imply a nonstationary shock in Al. Therefore, in our case, shock velocity was determined by measuring the time difference between shock breakout on the rear side of the Al flat layer (base), and the arrival of the laser pulse on the target front side.

EXPERIMENTAL RESULTS

The streak camera image in Fig. 3 shows the breakout from a stepped Al target (base and step thickness were both 5 μm). In this particular shot, an average shock velocity $D=29.6$ μm/ns was measured, by simply dividing the step thickness by the shock transit time in the step.

The fiducial on the upper-left part of Fig. 3, was absolutely synchronized (with a fixed time difference of 29 ps) to the arrival of the laser pulse on the front surface of the target. Hence, as said above, the shock velocity can also be obtained by the time difference between the fiducial and the shock breakout on the target rear side. Of course this measurement is *not* direct because, at early times, the motion of the shock front is nonstationary going through an acceleration phase [16]. However we verified that by using the numerical code MULTI [17], we could well reproduce both the experimental shock transit time in the step (and then the shock velocity) and the absolute time difference between fiducial and shock breakout *at the same time* (the difference between experimental and numerical values falling well within our experimental error bars). This comparison was important because, in the case of multilayered targets, the shock velocity in Al

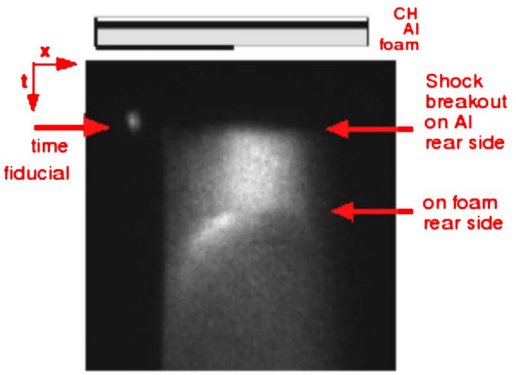

FIG. 4. (Color online) Shock breakout image from an Al/foam target for laser energy $E_L=215$ J and a foam density $\rho_0=0.055$ g/cm^3 (target scheme on the top). Image size is 10 ns$\times$1300 μm. Time flows up to down. The time between the fiducial maximum and the breakout on Al rear is $\Delta t=9$ ps. We did run MULTI simulations by adjusting the laser intensity so to obtain the same fiducial-to-shock delay as in the experiment. These showed that a stationary value of the shock velocity ($D_{\mathrm{Al}}=33.9$ μm/ns) was reached in the last 2 μm of the Al base. The time between shock breakouts on Al and foam is $\Delta t=3088$ ps giving $D_{\mathrm{foam}}=59.9$ μm/ns (foam thickness was 185 μm on this shot).

was indeed measured only via the indirect method (see Fig. 4). In other words, the comparison between experimental and numerical results provided a validation of such method.

Figure 4 shows instead a streak image from an Al/foam target (in this case only, the target front was not covered by the CH layer). All other shots were realized with a 4.9 ns window (instead of 10 ns) in order to increase the accuracy of the measurement. The left-hand side of the target rear is covered with a very thin Al layer. When the shock reaches the Al rear side, its breakout produces a strong luminosity, which is detected through the transparent foam (but it is partially masked on the left by the thin Al layer). On the contrary the luminosity due to the shock breakout on the foam rear side is strongly enhanced on the left by the presence of the Al thin layer.

Some curvature of the shock front at the edges is evident when it breaks out from the foam. This is due to the large foam thickness, which begins to be no longer negligible with respect to the focal spot size. However, the shock front in the central part of the image appears still to be reasonably flat. This was confirmed by performing simulations with the codes MULTI2D [18] and DUED [19], by which we also verified that the change in shock velocity with respect to the 1D case is negligible in our experimental conditions. They also allowed checking that the shock velocity is stationary in the foam.

Figures 5 and 6 show our experimental results for four different initial foam densities (ρ_0 from 0.055 to 0.130 g/cm^3). They are compared to the respective shock polars for a perfect gas, $P=[(\gamma+1)/2]\rho_0 U^2$ (continuous lines) [20]. All results are thermodynamically consistent, i.e., they are above the thermodynamical limits (dashed lines), where $D=U$ (or the density ρ of the compressed foam goes to ∞). Starting from the Rankine-Hugoniot relation expressing momentum conservation in the strong shock limit (i.e., $P=\rho_0 UD$), this is simply given by $P=\rho_0 U^2$. The error bars in the figures have been calculated by propagating the errors on target thickness and shock breakout time (± 62 ps when 4.9 ns window is used). On average these are of the order of 7% on U and 9% on P (notice that the error bars are asymmetric with respect to the experimental point).

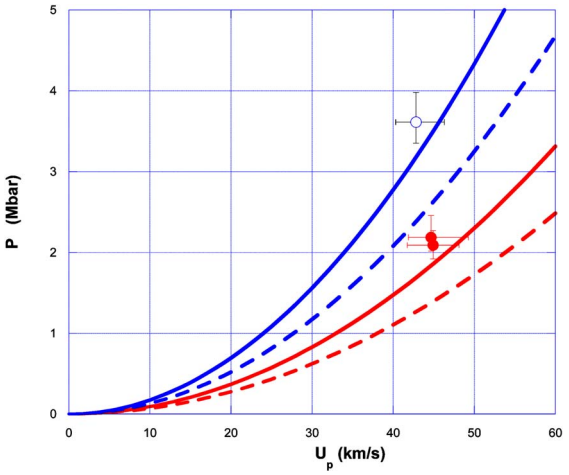

FIG. 5. (Color online) Our experimental results (circles) for $\rho_0=0.069$ g/cm^3 (red, full) and for $\rho_0=0.130$ g/cm^3 (blue, empty) compared to the respective shock polars for a perfect gas (continuous lines) and the thermodynamical limits (dashed lines).

From our experimental results it was also possible to deduce the acceleration factor ($g=U_{\mathrm{foam}}/U_{\mathrm{Al}}$) vs foam density (see Fig. 7). We compared our results to two different models. The first calculates the isentropic release curve, in the perfect gas approximation, of the Al plasma in the foam [21]. In this case the acceleration factor g must be calculated semianalytically, as described in Ref. [22]. The second one is a simple model based on the fact that, in first approximation,

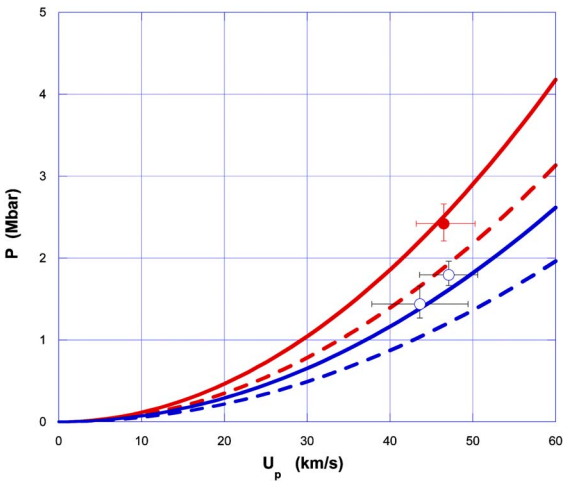

FIG. 6. (Color online) Our experimental results (circles) for $\rho_0=0.055$ g/cm^3 (red, full) and for $\rho_0=0.087$ g/cm^3 (blue, empty) compared to the respective shock polars for a perfect gas (continuous lines) and to the thermodynamical limits (dashed lines). The lower point for $\rho_0=0.055$ g/cm^3 corresponds to Fig. 4 and was obtained on a longer time window and no CH coating (this shot has larger error bars but it shows no larger deviation than the others, probably implying little influence of preheating).

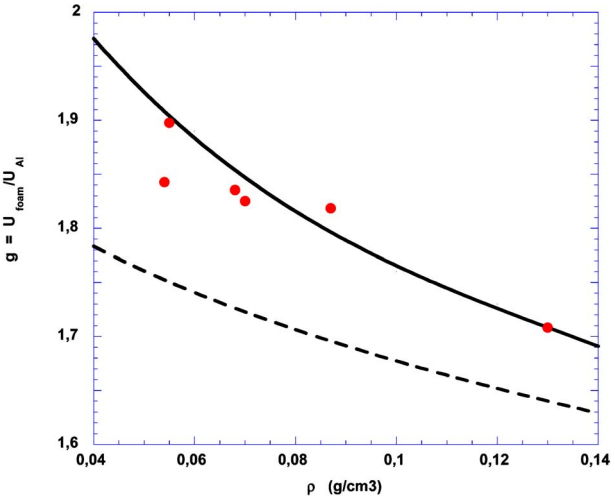

FIG. 7. (Color online) The acceleration factor ($\mathbf{g}=U_{\mathrm{foam}}/U_{\mathrm{Al}}$) from our experimental results (circles) vs foam density, compared to an "isentropic perfect gas" model (Ref. [21], continuous line) and to a "cold material–weak shock" model (Ref. [16], dashed line), in which the release isentropic is symmetric to the cold Hugoniot.

the release curve of Al is symmetric to the cold Hugoniot. Thereby this model applies to the case of cold materials and weak shocks [16,20]. In this last model, the acceleration factor is simply given by $g=2[1+(\rho_{0,\mathrm{foam}}/\rho_{0,\mathrm{Al}})^{0.5}]$.

Our results clearly show a much better agreement with the isentropic model. This is due to the fact that in the case of strong shocks, the limiting velocity of expansion of the free surface in vacuum is larger than what was found for cold materials and weak shocks, i.e., $2U_{\mathrm{Al}}$. Measuring shock acceleration at the interface between two materials, with a decreasing density jump, may have some relevance for astrophysics. Indeed in some astrophysical situations (i.e., the motion of the shock front in the atmosphere of a supernova) the shock is predicted to accelerate (and become hotter) as it propagates in a decreasing density profile. The case of a discontinuous density jump, may somewhat be considered as the limiting case of a continuous decreasing profile, therefore it is important to validate the physical laws for shock propagation in such a simple limiting case [21].

CONCLUSIONS

Pressure as high as 3.6 Mbar (previously unreached for such low density materials) were generated in the foams. Also this kind of foam, poly(4-methyl-1-pentene), was not used in the few previous experiments. Samples with four different values of initial density were used, so to explore a wider region of the phase diagram. Our results show that the shock polar for low-density foams at high pressure is close to that for a perfect gas with the same mass density. The shock-induced acceleration when the shock crosses the Al/foam interface was also measured vs foam density. Results are in close agreement with the predictions from a theoretical model, which calculates the isentropic release in the perfect gas approximation [21,22].

ACKNOWLEDGMENTS

Work performed at PALS with Financial support by Laserlab activity of the 6th Framework Programme of the E.U. (Contract No. RII3-CT-2003-506350), and partially by Grant No. LN00A100 of the Ministry of Education, Youth and Sports of the Czech Republic and by RFBR (Contract No. 03-02-17549). The authors thank C. Danson and D. Pepler, Rutherford Appleton Laboratory, for the PZP and acknowledge useful discussions with R. Ramis (Universidad Politecnica, Madrid), S. Atzeni (Università La Sapienza, Rome), and M. Koenig (LULI, CNRS, France).

[1] M. Desselberger *et al.*, Phys. Rev. Lett. **74**, 2961 (1995); R. G. Watt *et al.*, Phys. Plasmas **4**, 1379 (1997).
[2] M. Dunne *et al.*, Phys. Rev. Lett. **75**, 3858 (1995); D. Batani *et al.*, Phys. Rev. E **62**, 8573 (2000); T. Hall *et al.*, Laser Part. Beams **20**, 303 (2002); H. Nishimura *et al.*, Nucl. Fusion **40**, 547 (2000).
[3] J. Limpouch *et al.*, Plasma Phys. Controlled Fusion **46**, 1831 (2004); S. Yu. Gus'kov *et al.*, Laser Part. Beams **18**, 1 (2000).
[4] D. G. Colombant *et al.*, Phys. Plasmas **7**, 2046 (2000).
[5] D. Batani *et al.*, Plasma Phys. Controlled Fusion **40**, 1567 (1998); K. Takamatsu *et al.*, Phys. Rev. E **67**, 056406 (2003).
[6] B. Remington *et al.*, Phys. Plasmas **4**, 1994 (1997); R. P. Drake *et al.*, Phys. Rev. Lett. **81**, 2068 (1998); J. Massen *et al.*, Phys. Rev. E **50**, 5130 (1994).
[7] N. Holmes, Rev. Sci. Instrum. **62**, 1990 (1991); N. Holmes and E. See, in *Shock Compression of Condensed Matter*, edited by S. Schmidt *et al.* (Elsevier Science, New York, 1991), Vol. 1, p. 91.
[8] M. Koenig *et al.*, Phys. Plasmas **6**, 3296 (1999); **12**, 012706 (2005).
[9] D. Batani *et al.*, Phys. Rev. Lett. **92**, 065503 (2004); **88**, 235502 (2002); M. Koenig *et al.*, *ibid.* **74**, 2260 (1995); D. Batani *et al.*, Phys. Rev. B **61**, 9287 (2000).
[10] SESAME Report on the Los Alamos Equation-of-State library, Report No. LALP-83-4, T4 Group, Los Alamos, 1983.
[11] K. Jungwirth *et al.*, Phys. Plasmas **8**, 2495 (2001).
[12] D. Batani *et al.*, Phys. Rev. E **68**, 067403 (2003).
[13] R. M. Stevenson *et al.*, Opt. Lett. **19**, 363 (1994); M. Koenig *et al.*, Phys. Rev. E **50**, R3314 (1994); D. Batani, C. Bleu, and Th. Lower, Eur. Phys. J. D **19**, 231 (2002).
[14] K. Nagai and B.-R. Cho, Jpn. J. Appl. Phys., Part 2 **41**, L431 (2002); S. Okihara *et al.*, Phys. Rev. E **69**, 026401 (2004); K. Nagai *et al.*, Fusion Sci. Technol. **45**, 79 (2004); Jpn. J. Appl. Phys., Part 2 **41**, L1184 (2002).
[15] A. Benuzzi *et al.*, Phys. Plasmas **5**, 2410 (1998).
[16] D. Batani *et al.*, Phys. Rev. E **63**, 046410 (2001).
[17] R. Ramis *et al.*, Comput. Phys. Commun. **49**, 475 (1988).
[18] R. Ramis and J. Meyer-ter-Vehn, MULTI2D—A Computer Code for two-dimensional radiation hydrodynamics, MPQ-174, 1992.
[19] S. Atzeni, Comput. Phys. Commun. **43**, 107 (1986).
[20] Y. B. Zeldovich and Y. P. Raizer, *Physics of Shock Waves and High Temperature Hydrodynamic Phenomena* (Academic, New York, 1967).
[21] R. Teyssier, D. Ryutov, and B. Remington, Astrophys. J., Suppl. Ser. **127**, 503 (2000).
[22] M. Koenig *et al.*, Appl. Phys. Lett. **75**, 3026 (1999).